scientific reports

Check for updates

OPEN

Microneedle patch casting using a micromachined carbon master for enhanced drug delivery

Hye Jin Choi[1,6], Asad Ullah[2,6], Mi Jin Jang[3], Ui Seok Lee[4], Min Chul Shin[1], Sang Hyun An[3], Dongseon Kim[3], Bo Hyun Kim[5]✉ & Gyu Man Kim[1]✉

For successful treatment of diseases, sufficient therapeutics must be provided to the body. Microneedle applications in therapeutic delivery and analytics sampling are restricted because of various issues, including smaller area for drug loading and analytics sampling. To achieve sufficient drug loading and analytics sampling and improve drug penetration while maintaining painless administration, patch-type microneedle arrays were designed and fabricated using polymer casting from a conical cavity mold. Microcavities were formed on a carbon plate via micromechanical machining. A porous polymer layer was coated on a microneedle patch (MNP). The pores of the porous polymer layer provided space and channels for drug delivery. A pH-sensitive polymer layer was employed to cap the porous polymer layer, which prevented drug leakage during storage and provided a stimulus drug release in response to body pH conditions. The drug can be delivered through holes connected to both sides of the patch. The drug release of the MNP was investigated in vitro and in vivo and showed conceptual proof that these MNs have the potential to enhance treatment protocols for various diseases with the flexibility of coating and therapeutic materials and offer significant scope for further variations and advancement.

Keywords Microneedles, Porous polymer coating, Stimulus release, Micromechanical machining

Transdermal drugs are medications delivered through the skin. This type of drug delivery system allows for the controlled release of the medication over an extended period[1]. Transdermal drug patches are commonly used to treat conditions such as chronic pain, osteoarthritis, nicotine addiction, and hormone replacement therapy. The medication is typically stored in a reservoir within the patch and is released through the skin using a combination of diffusion and iontophoresis, which is the application of a small electric current to enhance the transport of the medication through the skin. Transdermal drug patches can provide a steady consistent dose of medication, which can improve efficacy and reduce the risk of side effects compared with oral or injectable forms of the same medication[2,3].

Microneedles (MNs) are miniaturized medical devices that contain an array of micronized needles. They are small, typically less than 1 mm in length, needles used for transdermal drug delivery. They are designed to penetrate the upper layers of the skin (stratum corneum) without reaching nerve endings and blood vessels, which reduces the pain and bleeding associated with traditional hypodermic needles[4,5]. They are a minimally invasive drug delivery system that can be used to administer drugs painlessly and take samples for investigation. They are mild and less harmful to the human body and are easy for medical staff and patients to use[5]. MNs can be made from various materials, such as metal, silicon, and biodegradable polymers. They can be arranged in various configurations, including arrays, patches, and solid structures[6].

MNs can enhance the transport of drugs across the skin by creating small channels through the stratum corneum, which allows for increased drug diffusion[7]. They have many advantages over traditional hypodermic needles, such as being easy to use, painless, and minimally invasive and having a higher patient acceptance[8,9]. They also have the potential to reduce needle stick injuries and cross contamination, which makes them safer

[1]School of Mechanical Engineering, Kyungpook National University, Daegu 41566, South Korea. [2]Department of Mechanical Engineering, University of Engineering and Technology, Mardan, Khyber Pakhtunkhwa 23200, Pakistan. [3]Preclinical Research Center, Daegu Gyeongbuk Medical Innovation Foundation, Daegu 41061, South Korea. [4]Department of Mechanical Engineering, Graduate School, Soongsil University, 369 Sangdo-ro, Dongjak-gu, Seoul 06978, Republic of Korea. [5]School of Mechanical Engineering, Soongsil University, Seoul 06978, South Korea. [6]These authors contributed equally: Hye Jin Choi and Asad Ullah. ✉email: bhkim@ssu.ac.kr; gyuman.kim@knu.ac.kr

for both patients and healthcare workers. MNs have the potential for use in various applications, including real-time biomarker detection[10]. They can be used to efficiently deliver drugs, vaccines, insulin for diabetes, cancer therapeutics, proteins, small molecules, liquid drugs, and other biomolecules to multiple parts of the human body for disease treatment[11,12]. They can also be used in paper chips, microfluidic systems, and other techniques for sensitive detection[13,14]. In addition, they can carry cells and facilitate cell culture, cytology tests, cytokine delivery, and more[15,16]. They are also being researched for use in cosmetics and skin care products and in gene therapy along with painless blood sampling[17–20]. There is growing interest in developing new-generation "smart MNs" that are bionic, bioderived, or biocompatible and have unique properties, such as skin adhesion, dissolvability, responsiveness, and tip–substrate detachability, to meet the demands of different application scenarios, such as wearable devices, rapid delivery, responsive delivery or detection, and sustained delivery[21].

From the perspective of transdermal drug delivery, porous materials play a crucial role in the development of effective and efficient transdermal patches. These materials are utilized in transdermal patches to enhance drug permeation through the skin. The pores within these materials act as channels for the drug to pass through the skin and reach the bloodstream. Furthermore, porous materials increase the surface area of the patch, thereby allowing for a greater amount of drug to be delivered[22]. One of the key challenges in developing transdermal patches is controlling the release of the drug. Porous materials address this challenge by regulating the size and shape of the pores, as well as the surface area of the patch. This control can be achieved by employing various types of polymers, such as hydrogels, which enable the controlled release of drugs over time[23].

Previously, our research team developed a smart MN using a simple approach of coating a porous polymer layer on stainless-steel MNs (SS-MNs) and applied it to glucose-responsive insulin delivery and smart drug delivery for wound healing[24–26]. SS-MNs have the advantages of being biocompatible and easy to manufacture and especially having high mechanical strength. However, when using stainless steel as a material for MNs, the "poke and pull" method is inconvenient, and the sharp tip remains after use, generating medical waste. Above all, it is difficult to load drugs directly onto SS-MNs. Therefore, our research team proposed a surface porous coating method as a means to load drugs onto SS-MNs[9]. However, this method has the disadvantage of not being able to accommodate a large amount of drugs. Therefore, to overcome this limitation, MNs using polymers instead of metals were manufactured to dissolve in the body, thereby eliminating the generation of medical waste and relatively increasing the drug loading. In addition, an approach capable of multiple-drug delivery is presented. Polymer MN fabrication methods vary depending on the polymer properties, but the most used method is micromolding, which requires a mold. Manufacturing methods for molds include photolithography, laser processing, and 3D printing. However, photolithography requires complex processes to produce molds of various shapes and sizes. Laser processing and 3D printing have low shape accuracy for micromolds[27]. In this study, micromechanical machining was used to make an MN mold. Micromechanical machining is a relatively simple process compared to other processes and allows the production of micromolds of various shapes at low cost[28,29]. As the mold material, fine-grain carbon with high purity was used. Because it is a brittle material, burrs are not generated during mechanical machining, making it advantageous for machining micromolds[30]. Here, the smart functions implemented in the previously reported SS-MNs were applied to the new polymer MNs and manufactured using a new approach that has not been previously attempted.

To achieve sufficient drug loading and analytics sampling and improve drug penetration while maintaining painless administration, we designed two types of MN arrays in patch shape to provide active and passive stimulus drug delivery with increased therapeutics. In the first array, we fabricated porous polymer coatings on the MNs and the base of the patch, which increased the loading efficiency and provided automatic "drug release" in response to body pH conditions. The pores of the porous polymer layer entrapped the drug and provided channels for drug flow. The MNs and base were coated with a stimulus-responsive polymer. Upon insertion into the body, the responsive MN coating was dissolved by the body interstitial fluid, and the loaded drug was released in response to the body stimulation. Upon dissolution of the protective coating on the MN periphery, the drug loaded on it defused in the body. Furthermore, the pores were interconnected, so the drug loaded on the MN base started flowing through these pores and diffused in the body. It exhibited three times more drug delivery efficiency than metallic MNs.

In the second array, the MNs were connected to the drug reservoir through holes punctured in the base of the MN array. The drug from the reservoir flowed through these holes into the porous base coating of the MN array and then through the pores of the porous coating of the MNs and diffused in the body. If this is combined with microfluidic chips or hydrogels, it can lead to expanded research, such as increasing drug loading and applying the release of two or more types of drugs. Thus, we achieved continuous drug flow using a simple and cheaper fabrication method.

Materials and methods

Materials

The chemicals used in this study were purchased from Sigma-Aldrich (unless mentioned otherwise): dichloromethane (DCM; anhydrous, ≥ 99.8%, ρ: 1.325 g/mL, MW: 84.93 g/mol, mp: − 97 °C), poly(lactic-co-glycolic acid) (PLGA; lactide:glycolide = 65:35, MW: 40,000–75,000), polyvinyl alcohol (PVA; MW: 31,000–50,000, 98–99% hydrolyzed), lidocaine (MW: 234.34 Da), gelatin (from porcine skin), and phosphate-buffered saline (PBS). Eudragit S100 was gifted by Evonik Korea. Orient Bio Inc. (Seoul, South Korea) provided all hairless SKH-1 mice. Polycrystalline diamond (PCD) was used as the microtool material. A carbon plate was used as the master mold for the MNs.

Ethical statement

The in vivo experimental procedures were performed in accordance with the protocols approved by the Institutional Animal Care and Use Committee at the Experimental Animal Center of Daegu Gyeongbuk Medical Innovation Foundation, South Korea (DGMIF-20022501-00). All experiments were performed by relevant named guidelines, regulations, and the ARRIVE guidelines.

Fabrication of the carbon master mold and MN array casting

To overcome the deficiency of low drug loading associated with MN applications, we designed two types of master molds for MN casting. The first master mold was simple and targeted high drug delivery by enhancing the drug loading area of the MN array, while the second master mold achieved it through continuous drug flow from the reservoir located on the backside of the patch. The second master mold connected the MNs to the drug reservoir, which allowed the flow of the drug to the body through holes machined in the base of the MN array and then through the pores on the base of the MN array and the MN periphery.

The MNs' carbon master molds were fabricated using the machining process. Figure 1 shows a schematic of their manufacturing process. For the master molds of the MNs, conical cavities were machined using customized microtools, as shown in Fig. 2. In this study, microwire electrical discharge machining (WEDM) was used to fabricate the customized tools[27,28]. Since PCD, the tool material, has very high hardness and is useful for machining microfeatures on carbon plates without severe tool wear. The first master mold was designed by making 600-µm-deep conical cavities on the carbon plate using micromachining to fabricate the MN array. The tool rotational speed was 60,000 rpm, and it took approximately 1 min for each drilling. The second master mold, which connected the MNs to the drug reservoir, was designed by machining 100-µm square pins with a height of 200 µm on the upper side of the carbon master mold (Fig. 3). For the machining of square pins, a microcylindrical tool with a flat end was used.

Replication of the MN array started with PDMS casting from the carbon mold. Female PDMS molds were fabricated from the carbon master molds by inversely duplicating the master MN array using PDMS at a ratio of 10:1 of the prepolymer to the curing agent, followed by curing at 90 °C for 2 h. The PDMS mold separated from the carbon mold was in the form of an MN array, which served as the first replica for the fabrication of a second PDMS mold. To facilitate easy separation from the PDMS replica, the surface was treated with a PEG (Polyethylene Glycol) solution. The second PDMS casting was then carried out. After curing, the second (2nd) PDMS mold and the PDMS replica were carefully separated, resulting in the final mold for MN fabrication.

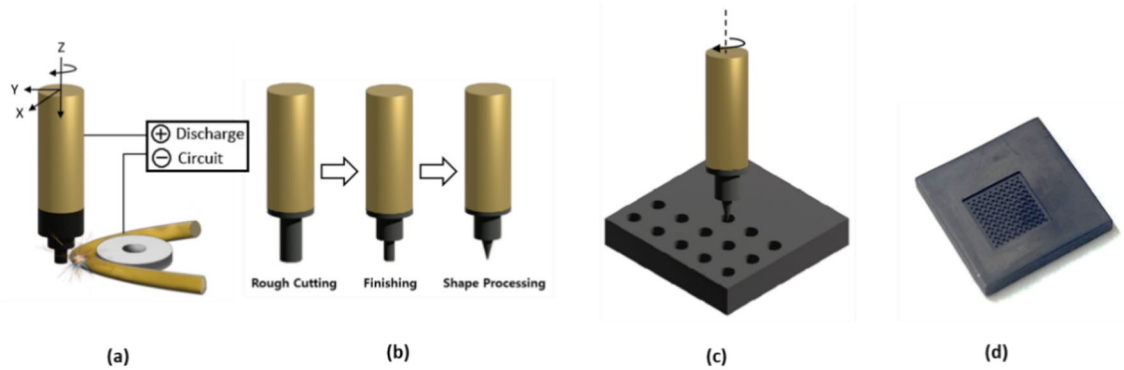

Figure 1. Schematic and optical image of the carbon mold manufacturing process using the machining process. Schematic of (**a** and **b**) the PCD tool manufacturing process using micro-WEDM and (**c**) the carbon mold fabrication process using the customized microtools. (**d**) Optical image of the fabricated carbon mold.

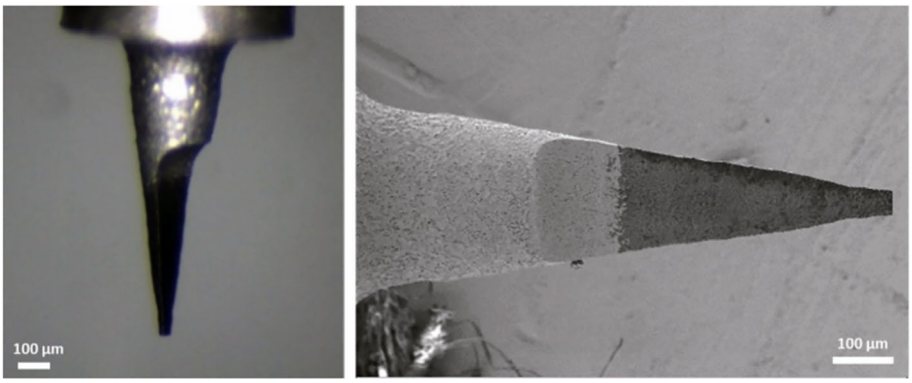

Figure 2. Customized microtool for conical cavity machining.

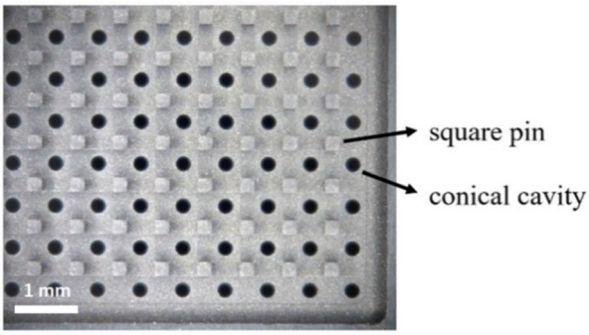

Figure 3. Master mold with conical cavities and square pins.

Then, the PVA MN array was replicated from the 2nd PDMS mold. We arranged a 50% (w/v) PVA solution and poured it on the 2nd PDMS mold to fabricate the PVA MN array. In all, 10 g of powdered PVA was dissolved in 20 mL of deionized water at 90 °C, forming a 50% (w/v) PVA solution that is transparent, amber, and thick. The MN array was cast using the 50% aqueous PVA solution by pouring it on the female PDMS mold consisting of a 10 × 10 array of MN cavities. To ensure filling of all cavities, centrifugation of the mold along with the PVA solution was conducted in a centrifugal homogenizer at 3000 rpm for 30 min. The MN array was dried at room temperature for one day, after which the excess PVA solution was removed. The MN array was carefully peeled from the mold and observed using stereomicroscopy prior to field-emission scanning electron microscopy (FE-SEM). The porous coating of the MN array was accomplished using the emulsification method, as explained in the next section. A schematic of the MN array fabrication from a carbon master mold is shown in Fig. 4. In this study, the first MN array was used for all subsequent application studies.

Preparation of the MNs for drug delivery

The MNs for drug delivery were prepared in two stages. In the first stage, a drug-containing polymer layer with a porous structure was coated on the PVA MN array. This process involved the following procedure. A 50-mL drug solution was emulsified in 4 mL of PLGA solution (2% w/v in DCM) at 20,000 rpm for 3 min to form the coating solution. The PVA MN array was manually dipped in the coating solution and removed. Thus, the drug was entrapped in the pores of the coating layer on the MNs and on the base of the MN array. In the second stage, Eudragit S100, a pH-sensitive polymer that dissolves at alkaline pH, was dissolved in 3% (v/v) aqueous acetone to prepare a 7% (70 mg/mL) solution. The MNs from step I were dipped in the Eudragit S100 solution (70 mg/mL) to form the pH-responsive layer on the porous coating. Subsequently, the MN samples were maintained at room temperature for 120 min to ensure that the solvent completely evaporated and were washed with water to remove any residuals.

In vitro drug delivery of the MN array

The in vitro performance of the developed MN array for transdermal drug delivery was analyzed. Two samples were examined for this purpose. One sample containing 100 MNs was coated with a drug-containing layer on the MNs, while the other sample containing 100 MNs was coated with a drug-containing layer on the MNs and on the base of the MN array. Both samples were incubated in PBS for the same period, and the drug released was quantified using confocal microscopy, as reported in a previous study[24]. Samples were taken at fixed time intervals from both incubated MN arrays. The amount of drug released in the receptor solution was calculated

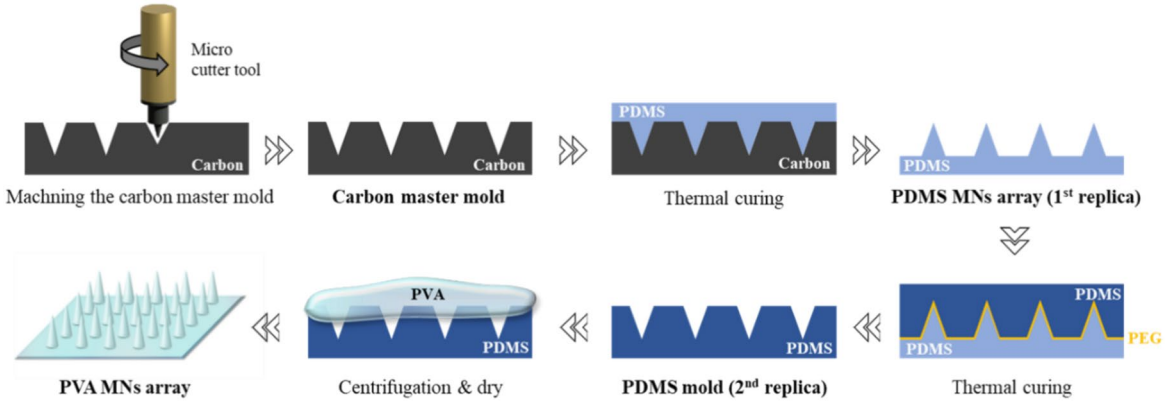

Figure 4. Schematic of the MN array fabrication process.

from the fluorescence intensity of the supernatant, and the results were plotted on a graph to compare the drug release from both samples.

Drug delivery and insertion capability of MNs in animals

The in vivo experimental procedures were performed in accordance with the protocols approved by the Institutional Animal Care and Use Committee at the Experimental Animal Center of Daegu Gyeongbuk Medical Innovation Foundation, South Korea (DGMIF-20022501-00). The hairless SKH-1 mice were anesthetized using isoflurane (1–2%). Then, Alexa Fluor 680 (AF680)-loaded MNs were applied to the dorsal skin of the mouse. In vivo fluorescence images were obtained using an in vivo imaging system (IVIS SpectrumCT, PerkinElmer). A filter set with excitation and emission wavelengths of 675 and 720 nm, respectively, was used to measure the fluorescent signal of AF680.

Results and discussion

Master mold and MN fabrication results

Among the issues related to MN applications, smaller area for drug loading and analytics sampling on MNs is the main issue. Various attempts were made by the researchers to handle this issue. This work presents a simple approach to increase the drug loading area. The drug loading area was increased by coating a porous polymeric layer on the MN peripheries and on the base of the MN array while keeping the size of the MNs and the MN array fixed. The MN array mold was fabricated using micromachining to create 600-µm-deep conical cavities on the carbon plate. Figure 5a shows 100 conical cavities with top and bottom diameters of 250 and 30 µm, respectively, a length of 600 µm, and an interval of 400 µm base-to-base, which were engineered on the carbon master mold. Figure 5b shows the entrance hole with a diameter of 250 µm. Figure 5c shows the cavity profile with a depth of 600 µm, which was measured by a confocal laser microscope (OLS-5000, Olympus Inc.). In the second master mold, a microcylindrical tool with a flat end was used to machine square pins between the needle arrays. Figure 6 shows an observation of the manufactured first and second carbon master molds, respectively.

Female PDMS molds were fabricated from the carbon master molds by inversely duplicating the master MN arrays using PDMS at a ratio of 10:1 of the prepolymer to the curing agent, followed by curing at 90 °C for 2 h. Then, the 50% (w/v) PVA solution was used to fabricate the PVA MN array. The resulting MNs were arranged in a 10 × 10 array with intervals of 400 µm. The diameters of the MNs at the base and top were 250 and 30 µm, respectively, with a length of 600 µm. The thickness of the porous coating was 15–20 µm. The second MN array was also arranged in 10 × 10 with intervals of 400 µm. The diameters of the MNs at the base and top were 250 and 30 µm, respectively, with a length of 600 µm. In addition, it contained 100-µm square holes with a height of 200 µm distributed on the base, which connected the MNs to the drug reservoir, allowing drug flow through these holes and then through the pores on the base of the MN array and the MN periphery to the body. Two different shapes of the MN array were observed at each stage, as shown in Figure 7. Figure 7a and b display the first and second MN arrays, respectively. Figure 8a and b show their FE-SEM images at different magnifications without and with the porous coating, respectively. All MNs had the same size and were smoothly coated with a smart porous drug-containing layer on the MN surfaces and on the base of the MN array. Additionally, for the successful and appropriate clinical application of microneedles (MNs), they must be inserted into the skin without bending or breaking. Therefore, the mechanical strength of microneedles is a critical factor influencing their ability to penetrate the skin[31]. Therefore, the strength was measured by applying pressure to the tip of the microneedle at a rate of 0.1 mm/sec using a universal testing machine (UTM; 3400 series, Instron, Norwood, MA, USA). As shown in Figure 8c, the prepared MNs could withstand a force of 1N per needle, which exceeds the force required for human skin insertion (0.1N), indicating high mechanical strength[32].

In vitro stimulus drug release of the MN array with the porous coating

Two samples were prepared for comparison in the in vitro analysis. In the first sample, a porous-coated SS-MN, the drug was entrapped in the pores of the porous polymer coating only on the MNs, while in the second sample which was the polymer MN developed in this study, the porous polymer coating was applied to the MN body and

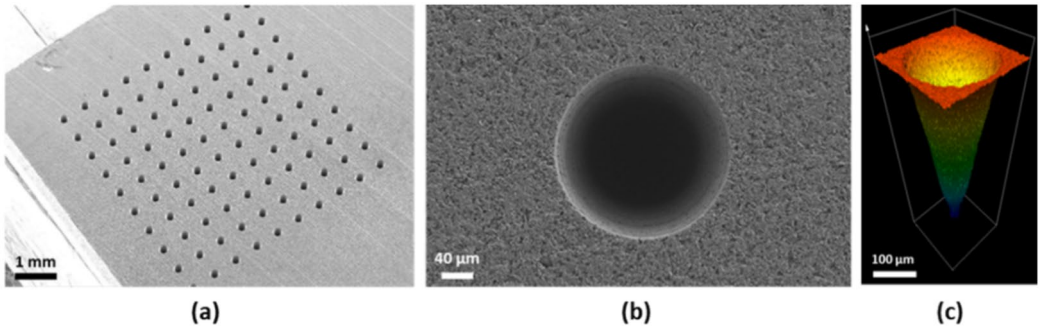

Figure 5. (**a**) SEM image of the micro conical cavities machined on the carbon plate, (**b**) entrance hole, and (**c**) cavity profile.

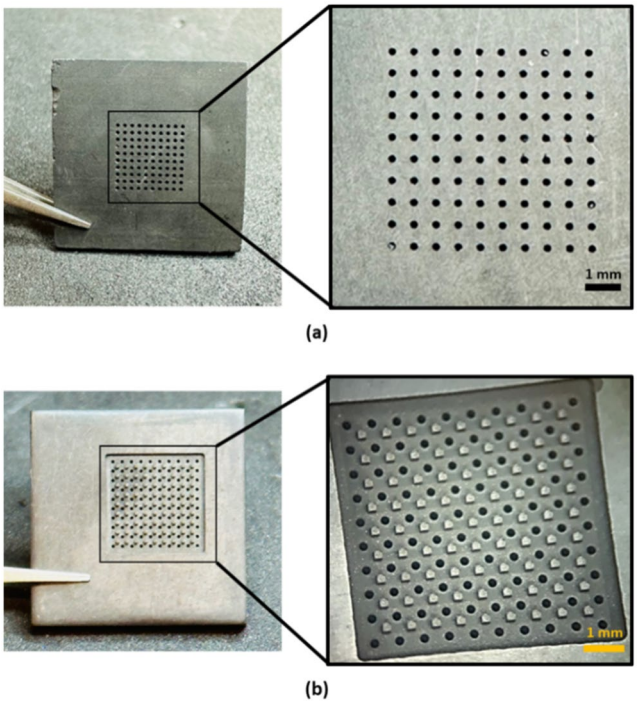

Figure 6. Optical images of the (**a**) first and (**b**) second carbon master molds.

to the base of the MN array. Both samples were incubated in PBS to analyze the release of the loaded drug. The parameters of the receiving medium were set to represent the body environment, i.e. 37 °C with a pH level of 4.5, which is the pH for healthy skin[33]. At predefined time intervals, samples were taken from the culture medium to monitor the diffusion of drug release. According to theoretical calculations, the volumes of the coated areas of SS-MN and PVA MN bodies were estimated to be approximately 0.16 mm^3 and 0.21 mm^3, respectively. In the case of SS-MN, coating the base of the microneedle was challenging due to its inherent properties. Conversely, polymer MNs could be coated up to the base, resulting in estimated total volume of coated area of approximately 0.895 mm^3. For PVA MNs, the porous coating extended to both the microneedle body and base, thereby increasing the total volume of coated area by about four times compared to coating only the needle body. This increase was closely related to drug loading efficiency, as the porous polymer layer's surface area directly correlated with the region available for drug entrapment. As depicted in Fig. 9a, the experimental results supported these theoretical predictions. When the coating was applied only to the needle portion of the microneedle (MN) array, the amount of drug released was less compared to when both the MN and the base of the MN array were coated. Specifically, the amount of drug released was approximately three times higher when the porous coating extended to the base compared to coating only the needle portion. Thus, it was confirmed that the PVA MNs fabricated in this study, with porous coatings applied to both the base of the array and the needle body, exhibited enhanced drug loading and release efficiency compared to SS-MNs. However, there is a discrepancy between the theoretical calculations and the experimental results. The theoretical calculations represent the volume of the area to be coated. In practice, however, drug loading is conducted after the porous coating is applied, which can result in differences in the amount of drug loaded onto SS and PVA MNs. It differs from drug patches in the way that, in patch application, some portion of the drug flows from the patches through the voids punctured by solid MN application into the skin, while a large portion of the drug remains on the surface of the skin due to the reclosing of the voids punctured by solid MNs.

In this work, the drug was entrapped in the pores of the porous coating on the MN surface and the base of the MN array. With the application of the MN array to the body, the responsive MN coating was dissolved by the body interstitial fluid, and the loaded drug was released in response to the body stimulation, while the base coating remained intact because of no stimulation. After the dissolution of the protective coating, the drug diffused in the body from the MN surface coating and then from the base coating because the pores were interconnected. Thus, all portions of the drug loaded on the MNs diffused in the body. Upon the application of the MN array, the protective coating on the MN peripheries dissolved in the skin, and the drug diffused in the body. In this way, we increased the efficiency of the MN array. Additionally, in this study, a pH-responsive polymer layer was coated over the porous layer to protect drug release and ensure that the drug was released only in specific pH environments. The efficacy of the developed MNs was analyzed under two different pH conditions, 4.5 and 7.5 (Fig. 9b). It was confirmed that a small amount of drug, approximately 30%, was released at pH 4.5. In contrast, exposing the MNs to a pH of 7.5 resulted in a significant increase in drug release. This demonstrates the pH-dependent release of the encapsulated drug from the developed MNs.

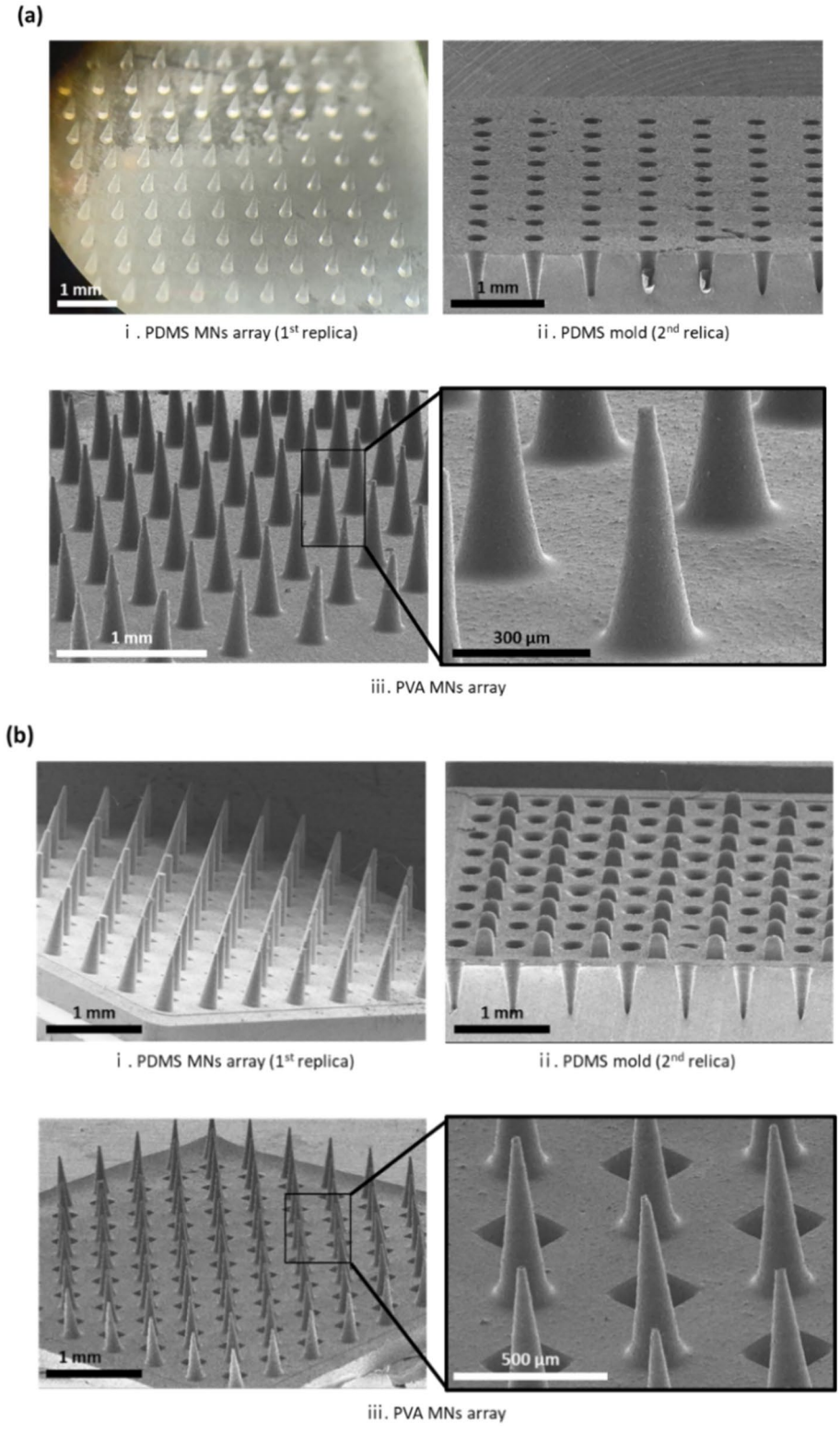

Figure 7. FE-SEM images of the fabrication steps from the carbon mold to the PVA MN array of two different shapes: (**a**) first MN array and (**b**) second MN array.

Drug delivery and insertion capability of MNs in animals

To determine whether the PVA MNs (first) had the appropriate strength to penetrate the skin and pH-responsive drug release properties, the MNs were applied to the dorsal skin of the SKH-1 mouse. For in vivo imaging, AF680,

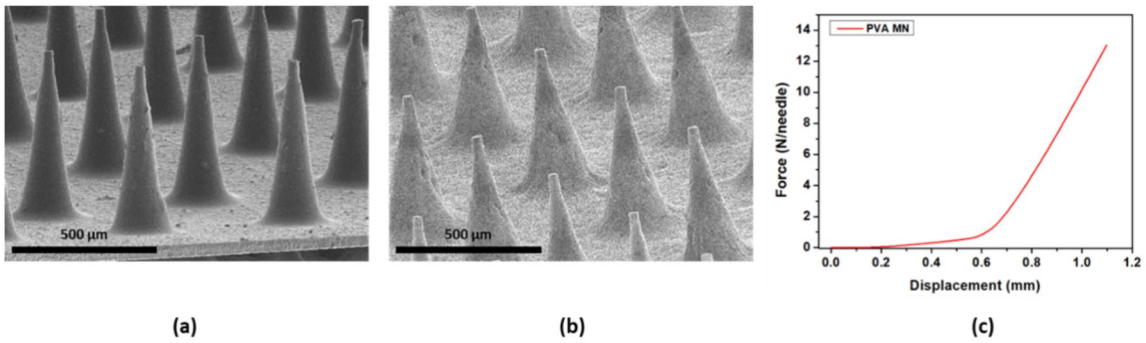

Figure 8. FE-SEM images of the MNs (**a**,**b**). (**a**) MN array without the porous coating. (**b**) MN array containing therapeutics in the pores after coating the Eudragit S100 film. (**c**) Mechanical behavior diagram of a PVA MN patch under vertical force.

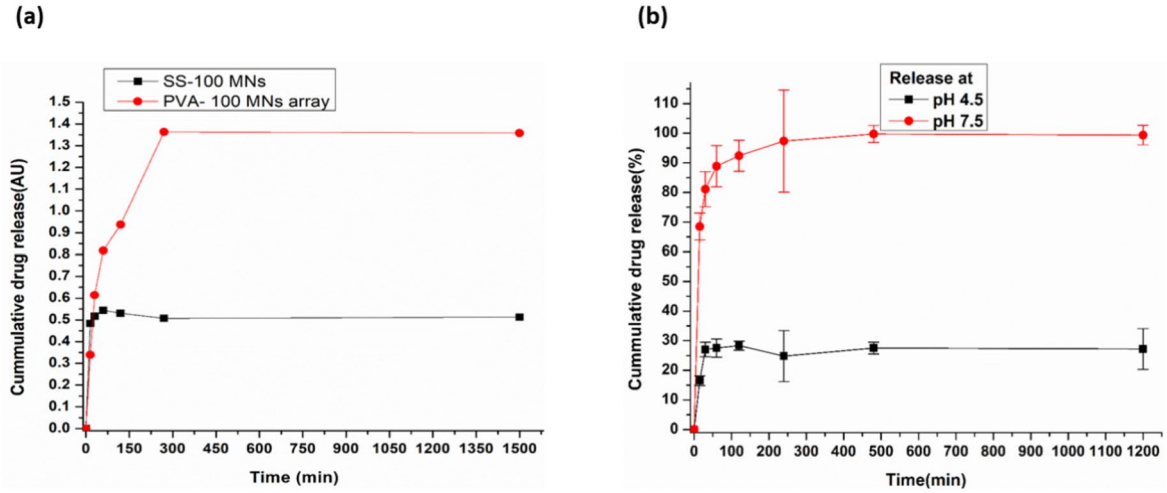

Figure 9. (**a**) Comparison of the release profiles of the drug for MNs cultivated in the liquid culture medium coated with and without the base of the MN array with physiological body conditions, i.e. healthy skin pH (pH 4.5) at 37 °C. (**b**) Release profile of the drug for wound pH-sensitive PVA MNs cultivated in the liquid culture medium with different pH values to mimic wound pH (pH 7.4) and healthy skin pH (pH 4.5) environment at 37 °C.

a near-infrared fluorescent dye used as a drug, was loaded in the MNs (0.25 mg/mL). As shown in Fig. 10a, two types of MNs coated and not coated with Eudragit S100 are applied to the dorsal skin of the mouse at the same pressure, and it was confirmed that they were well attached. After 30 min, the MNs were removed, and the fluorescence image was obtained by IVIS SpectrumCT (Fig. 10b).

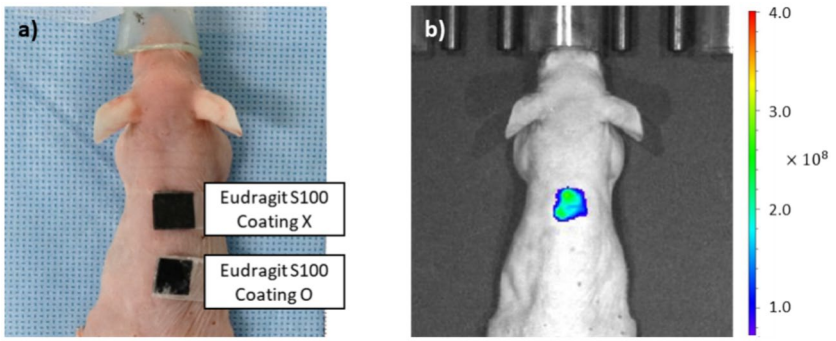

Figure 10. Images of (**a**) the application of two types of MNs on the dorsal skin of the mouse and (**b**) the IVIS SpectrumCT results.

Eudragit S100 is a pH-sensitive polymer that dissolves at alkaline pH (i.e. above pH 7) and is insoluble in an acidic microenvironment[34]. Therefore, fluorescence was detected at the sites where the uncoated MNs were applied, indicating that the MNs were sharp and hard enough to penetrate the skin without causing any bleeding or undesired skin abrasion. The MNs coated with Eudragit S100 did not show fluorescent signals because healthy skin has a slightly acidic pH. Thus, the MNs coated with Eudragit S100 have pH-responsive properties and can be used to treat skin diseases that exhibit alkaline conditions, such as skin wounds and atopic dermatitis.

Conclusion

In this study, two types of MN arrays in patch form were designed and fabricated to achieve sufficient drug loading and analytics sampling and improve drug penetration while maintaining painless administration. We presented a simple approach to increase the drug loading area, fixing the size of the MNs and the MN array by coating a porous polymer layer not only at the base of the MN array but also around the MNs. In this novel approach, the mold was fabricated by forming microcavities on a carbon plate using micromachining. A customized tool was fabricated using micro-WEDM, and a conical cavity was machined using the fabricated customized tool. The first master mold was designed by creating 600-µm-deep conical cavities on a carbon plate using micromachining to fabricate the MN array. In the second master mold, square pins were machined on the top surface of the carbon master mold to connect the MNs to the drug reservoir. A microcylindrical tool with a flat end was used to machine the square pins between the needle arrays. Patch-type PVA MNs were produced through polymer casting in each fabricated master mold. It was first coated with a porous polymer, and the pores of the porous polymer layer captured the drug and provided channels for drug flow. In this study, a pH-sensitive polymer was coated on the porous polymer layer to add an automatic drug release function in response to body pH conditions. The drug release of the final fabricated MNPs was investigated in vitro and in vivo. The first master mold achieved simple, targeted, and high drug delivery by enhancing the drug loading area of the MN array, whereas the second master mold achieved this through continuous drug flow from the reservoir located on the back of the patch. If this is combined with microfluidic chips or hydrogels, this could lead to expanded research, including increased drug loading and the application of releasing two or more types of drugs. In addition, we have shown proof of concept that these MNs have the potential to improve treatment protocols for various diseases and offer significant scope for further modifications and advancements.

Data availability

The datasets used and/or analysed during the current study available from the corresponding author on reasonable request.

Received: 11 April 2024; Accepted: 16 August 2024
Published online: 20 August 2024

References

1. Kakkar, S. & Singh, R. A review on transdermal drug delivery system. *Innorig. Int. J. Sci.* **3**, 1–5 (2016).
2. Tanwar, H. & Sachdeva, R. Transdermal drug delivery system: A review. *Int. J. Pharm. Sci. Res.* **7**, 2274 (2016).
3. Akhtar, N., Singh, V., Yusuf, M. & Khan, R. A. Non-invasive drug delivery technology: Development and current status of transdermal drug delivery devices, techniques and biomedical applications. *Biomed. Eng. Biomed. Tech.* **65**, 243–272 (2020).
4. Zhang, X., Wang, Y., Chi, J. & Zhao, Y. Smart microneedles for therapy and diagnosis. *Research* https://doi.org/10.34133/2020/7462915 (2020).
5. Mandal, A. *et al.* Cell and fluid sampling microneedle patches for monitoring skin-resident immunity. *Sci. Transl. Med.* **10**, eaar2227 (2018).
6. Aldawood, F. K., Andar, A. & Desai, S. A comprehensive review of microneedles: Types, materials, processes, characterizations and applications. *Polymers* **13**, 2815 (2021).
7. Wei-Ze, L. *et al.* Super-short solid silicon microneedles for transdermal drug delivery applications. *Int. J. Pharm.* **389**, 122–129 (2010).
8. Rad, Z. F., Prewett, P. D. & Davies, G. J. An overview of microneedle applications, materials, and fabrication methods. *Beilstein J. Nanotechnol.* **12**, 1034–1046 (2021).
9. Ullah, A., Kim, C. M. & Kim, G. M. Porous polymer coatings on metal microneedles for enhanced drug delivery. *R. Soc. Open Sci.* **5**, 171609 (2018).
10. Teymourian, H., Tehrani, F., Mahato, K. & Wang, J. Lab under the skin: Microneedle based wearable devices. *Adv. Healthc. Mater.* **10**, 2002255 (2021).
11. Yang, J., Liu, X., Fu, Y. & Song, Y. Recent advances of microneedles for biomedical applications: Drug delivery and beyond. *Acta Pharm. Sin. B* **9**, 469–483 (2019).
12. Xu, J. *et al.* Microneedle patch-mediated treatment of bacterial biofilms. *ACS Appl. Mater. Interfaces* **11**, 14640–14646 (2019).
13. Erdem, Ö., Eş, I., Akceoglu, G. A., Saylan, Y. & Inci, F. Recent advances in microneedle-based sensors for sampling, diagnosis and monitoring of chronic diseases. *Biosensors* **11**, 296 (2021).
14. Zhang, W. *et al.* Recent advances of microneedles and their application in disease treatment. *Int. J. Mol. Sci.* **23**, 2401 (2022).
15. Chen, B. Z., Zhao, Z. Q., Shahbazi, M.-A. & Guo, X. D. Microneedle-based technology for cell therapy: Current status and future directions. *Nanosc. Horiz.* **7**, 715–728 (2022).
16. Chang, H. *et al.* Cryomicroneedles for transdermal cell delivery. *Nat. Biomed. Eng.* **5**, 1008–1018 (2021).
17. McCrudden, M. T. *et al.* Microneedle applications in improving skin appearance. *Exp. Dermatol.* **24**, 561–566 (2015).
18. Sartawi, Z., Blackshields, C. & Faisal, W. Dissolving microneedles: Applications and growing therapeutic potential. *J. Control. Release* **348**, 186–205 (2022).
19. Blicharz, T. M. *et al.* Microneedle-based device for the one-step painless collection of capillary blood samples. *Nat. Biomed. Eng.* **2**, 151–157 (2018).
20. Lu, H., Zada, S., Yang, L. & Dong, H. Microneedle-based device for biological analysis. *Front. Bioeng. Biotechnol.* **10**, 851134 (2022).
21. Wang, Y., Wang, H., Zhu, X., Guan, Y. & Zhang, Y. Smart microneedle patches for rapid, and painless transdermal insulin delivery. *J. Mater. Chem. B* **8**, 9335–9342 (2020).
22. Liu, L., Kai, H., Nagamine, K., Ogawa, Y. & Nishizawa, M. Porous polymer microneedles with interconnecting microchannels for rapid fluid transport. *RSC Adv.* **6**, 48630–48635 (2016).

23. Liu, P. *et al.* Polymer microneedles with interconnected porous structures via a phase inversion route for transdermal medical applications. *J. Mater. Chem. B* **8**, 2032–2039 (2020).
24. Ullah, A. *et al.* Microneedle array with a pH-responsive polymer coating and its application in smart drug delivery for wound healing. *Sens. Actuators B Chem.* **345**, 130441 (2021).
25. Ullah, A., Choi, H. J., Jang, M., An, S. & Kim, G. M. Smart microneedles with porous polymer layer for glucose-responsive insulin delivery. *Pharmaceutics* **12**, 606 (2020).
26. Ullah, A., Kim, C. M. & Kim, G. M. Solvent effects on the porosity and size of porous PLGA microspheres using gelatin and PBS as porogens in a microfluidic flow-focusing device. *J. Nanosci. Nanotechnol.* **17**, 7775–7782 (2017).
27. Saha, B. *et al.* A review on the importance of surface coating of micro/nano-mold in micro/nano-molding processes. *J. Micromech. Microeng.* **26**, 013002 (2015).
28. Lee, P. A., Lee, U. S., Sim, D. B. & Kim, B. H. Microfluidic chip fabrication of fused silica using microgrinding. *Micromachines* **14**, 96 (2022).
29. Lee, P. A. & Kim, B. H. A study of microdrilling of fused silica using EDMed PCD tools. *Appl. Sci.* **12**, 11166 (2022).
30. Cho, Y., Hwang, J., Park, M.-S. & Kim, B. H. Fabrication methods for microscale 3D structures on silicon carbide. *Int. J. Precis. Eng. Manuf.* **23**, 1477–1502 (2022).
31. Yang, J. *et al.* Multifunctional hyaluronic acid microneedle patch embedded by cerium/zinc-based composites for accelerating diabetes wound healing. *Adv. Healthc. Mater.* **12**, 2300725 (2023).
32. Lv, H. *et al.* Collagen-based dissolving microneedles with flexible pedestals: A transdermal delivery system for both anti-aging and skin diseases. *Adv. Healthc. Mater.* **12**, 2203295 (2023).
33. Shi, L., Ramsay, S., Ermis, R. & Carson, D. pH in the bacteria-contaminated wound and its impact on *Clostridium histolyticum* collagenase activity: Implications for the use of collagenase wound debridement agents. *J. Wound Ostomy Cont. Nurs.* **38**, 514–521 (2011).
34. Ibekwe, V. C., Fadda, H. M., Parsons, G. E. & Basit, A. W. A comparative in vitro assessment of the drug release performance of pH-responsive polymers for ileo-colonic delivery. *Int. J. Pharm.* **308**, 52–60 (2006).

Acknowledgements

This research was supported by National Research Foundation of Korea (2022R1A6A3A01087329 and RS-2023-00208717) and the Technology Innovation Program (20010984) funded by the Ministry of Trade, Industry and Energy (MOTIE), Republic of Korea.

Author contributions

H.J.C. drafted the manuscript and performed the data analysis. A.U. conducted the experiment and wrote. M.J.J. S.H.A. and D.K design of animal experiments. U.S.L. fabricated the carbon maser mold. M.C.S helped supervise the project. G.M.K. and B.H.K. supervised the work and advised and edited the manuscript. All authors have approved the final version of the manuscript.

Competing interests

The authors declare no competing interests.

Additional information

Correspondence and requests for materials should be addressed to B.H.K. or G.M.K.